INDIAN INSTITUTE OF TECHNOLOGY KANPUR
DEPARTMENT OF MECHANICAL ENGINEERING

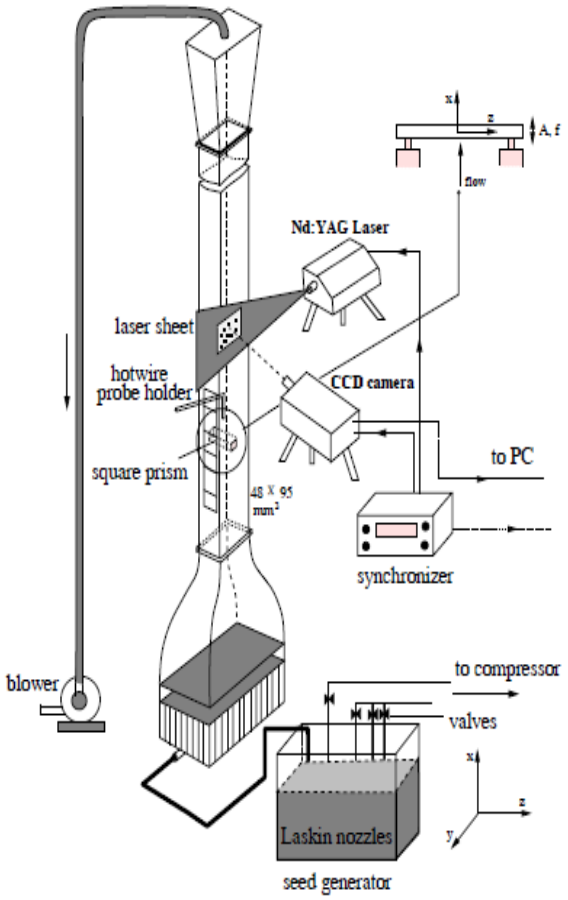

ME 231: FLUID MECHANICS LABORATORY

REPORT WRITING

All experiments in the Fluid Mechanics Laboratory require a formal report. The report should be written in such a way that anyone can replicate the performed experiment and obtain similar results. The reports should be simple and clearly written. Reports are due at the beginning of the every new laboratory turn. The report will communicate important ideas to the reader.

(1) Neatness: The experimenter is in effect trying to convince the reader that the experiment was performed in a straightforward manner with great care and with full attention to detail. A poorly written report might lead the reader to think that the experiment was carelessly performed.

(2) Organization: The reader will be able to easily follow each step discussed in the text.

(3) Accuracy: This will require checking and rechecking the calculations until necessary confidence is gained.

(4) Grammar: The report should be free of spelling and grammatical errors.

FORMAT OF REPORTS

Title Page – The title page carries the title and number of the experiment, date when the experiment was performed, names of students who participated in the experiment.

Table of Contents – Each page of the report must be numbered for this purpose.

Objectives – The objective is a clear concise statement explaining the purpose of the experiment. This is one of the most important parts of the laboratory report because everything included in the report must relate to the stated objective. The objective can be as short as one sentence and is written in the past tense.

Theory – The theory section contains a complete analytical development of all important equations pertinent to the experiment, and how these equations are used in the reduction of data. It should be written in text-book style.

Procedure –This section contains a schematic drawing of the experimental setup including all equipment used, their specification, and the manufacturer. Show the function of each part when necessary, for improving clarity. Describe how the experiment was performed in as much detail as necessary, with a view that somebody else can repeat the steps involved.

Results – The results section carries a formal analysis of the data with tables and graphs. The quality of plots should add to clarity in describing the outcome of the experiment.

Discussion and Conclusions – The interpretation of results will explain how the objectives of the experiment were fulfilled. If any analytical/empirical expression is to be verified, calculate the % error and account for it. Discuss this experiment with respect to its faults as well as its strong points. Suggest extensions of the experiment and improvements. Also recommend any changes necessary to better accomplish the objective.

Appendix

(1) Original date sheet (Get your data sheet signed by the instructor at the end of each experiment).

(2) Show how data were used by a sample calculation.

(3) Calibration curves of instrument, which was used in the performance of the experiment. Include manufacturer of the instrument, model and serial numbers. The instructor will usually supply calibration curves. Alternatively, calibration may be a part of the experiment.

(4) Bibliography listing all references used.

Short Report Format

Often the experiment requires not a formal report but an informal report. An informal report includes the **Title Page, Objectives, Procedure, Results** and **Conclusions**.

Graphs

In many instances, it is necessary to compose a plot in order to graphically present results. Graphs must be drawn neatly following a specific format. There are many software packages that have graphing capabilities. Nevertheless an acceptably drawn graph has several *features of note* as listed below.

- Border is drawn around the entire graph.
- Axis labels defined with symbols and units.
- Grid drawn using major axis divisions.
- Each trend is identified using a legend.
- Data points are identified with symbols.
- The line representing theoretical results has no visible data points.
- Nothing is drawn freehand.
- Figure caption is reasonably descriptive.

CLEANLINESS AND SAFETY

There are *housekeeping* rules that the user of the laboratory should be aware of and abide by. Equipment in the laboratory is delicate and it is important that it stays clean and dust does not accumulate within. The Fluid Mechanics Laboratory contains equipment that uses water, air or oil as the working fluid. In some cases, performing an experiment will inevitably allow water to get on the equipment and/or the floor. If no one cleans up the working area after performing an experiment, the laboratory would not be a comfortable or safe place to work in. No student appreciates walking up to and working with a piece of equipment that another student or group

of students has left in a mess. Consequently, students are required to clean up their area at the conclusion of the performance of an experiment. Cleanup will include removal of spilled water (or any liquid), and wiping the table top on which the equipment is mounted. The laboratory should always be as clean as, or cleaner than it was when you entered. Cleaning the lab is your responsibility as a user of the equipment. This is an act of courtesy that students who follow you will appreciate, and that you will also appreciate when you work with the equipment.

It is important to note that modern instruments are electronic devices and may involve optics, that as a rule, demands absolute cleanliness.

The layout of the equipment and storage cabinets in the Fluid Mechanics Laboratory involves resolving a variety of conflicting requirements. The goal is to implement safety requirements without impeding progress, but still allowing adequate workspace and necessary informal communication opportunities. Distance between adjacent pieces of equipment is determined by the need to allow enough space around the apparatus of interest. Every effort has been made to create a positive, clean, safety conscious atmosphere. Students are encouraged to handle equipment safely and to be aware of, and avoid being victims of hazardous situations.

NO BAGS ALLOWED IN THE LABORATORY PREMISES!

LIST OF EXPERIMENTS

i. Impact of jet on flat and curved surfaces

ii. Measurement of drag on a circular cylinder in high Reynolds number flow (wake survey method)

iii. Energy loss measurements in subcritical and supercritical open channel flow

iv. Measurement of fluid viscosity (air and oil)

v. Determination of friction factor as a function of Reynolds number in pipe flow

vi. Studying laminar-turbulent transition for flow in a tube

vii. Boundary layer flow over a flat plate

viii. Pressure distribution around a circular cylinder in high Reynolds number flow

EXPERIMENT 1: Jet impact on flat and curved surfaces

OBJECTIVES

1. Measure force acting on flat and curved surfaces as a function of jet velocity
2. Compare measured forces with those determined by using the integral form of the momentum equation.

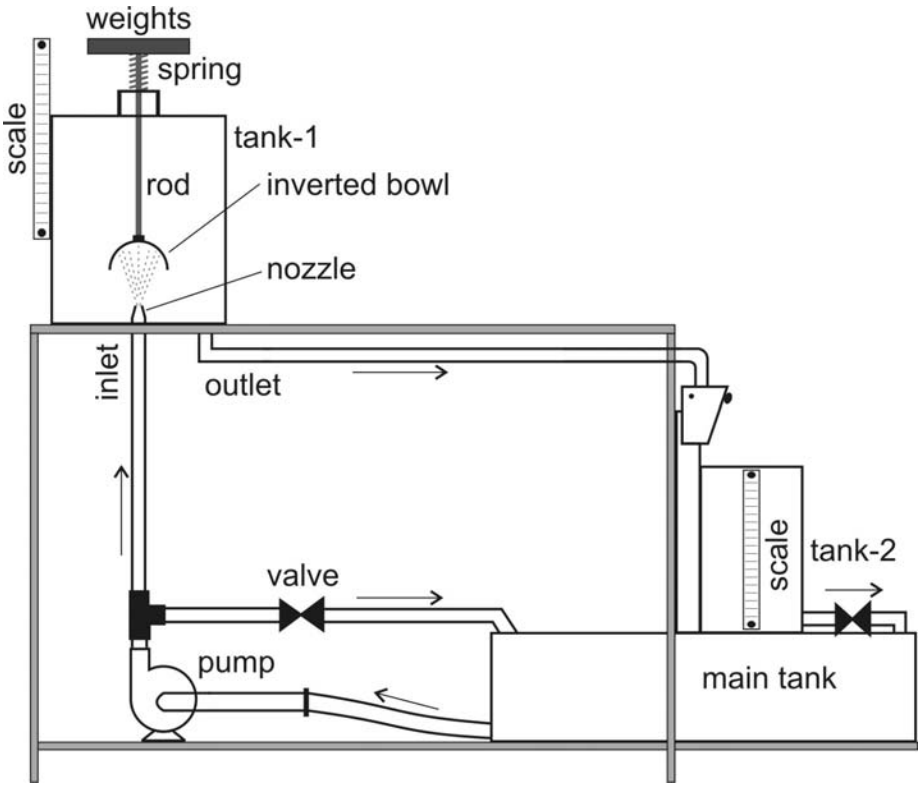

Figure 1: Impact of jet apparatus

The experimental set-up consists of a nozzle through which a water jet emerges in the vertically upward direction. The jet is visible through the transparent cover. It strikes the target surface positioned above it. The force generated by the jet can be measured by applying weights to balance the jet reaction. ACCOUNT FIRST FOR THE DEAD WEIGHT OF THE TARGET SURFACE AND THE CONNECTING ROD. Target surfaces are interchangeable, namely flat or curved.

The flow rate is determined by measuring the volume of water collected in the tank over a known period of time. Measure the geometric dimensions as needed for calculations.

Repeat the experiment for various flow rates and target shapes. Compare the experimentally determined forces in the vertical direction with those derived from the control volume formulation, namely (for a spherical cap):

$$F = 2\rho QU$$

Here ρ is the fluid density, Q is volume flow rate, and U is the average velocity of the fluid impacting the cap and nearly equal to that of flow leaving the nozzle. CORRECT FOR THE CHANGE IN THE IMPINGEMENT VELOCITY WITH THE VERTICAL COORDINATE. A slightly altered expression holds for force acting on the flat impacting surface.

Data sheet

Exit diameter of the nozzle: 8 mm
Cross-section of the collection tank: 244 × 394 mm^2
Mass of cup-rod-pan assembly 443 grams
Mass of flat piece-rod-pan assembly 318 grams
Mass of spring 12 grams

EXPERIMENT 2: Measurement of drag on a circular cylinder in high Reynolds number flow

Cylinders of varying diameter (d = 25.4 – 61 mm) are placed in a low speed wind tunnel. The force acting on them consists of viscous drag and form drag, the latter being predominant if flow separates on the surface of the cylinder. The wind tunnel provides velocities up to U = 15 m/s and for a diameter of 50 mm, the corresponding Reynolds number $=\rho Ud/\mu$ is 4.8×10^5. For a cylinder the laminar separated regime extends over $50 < Re < 5\times10^5$. Hence for the diameters and velocities studied here, the boundary-layer over the cylinder is expected to be laminar. Velocities below 1 m/s are difficult to attain in the wind tunnel without leading to unsteadiness in the approach flow.

Total drag can be measured by calculating the rate of loss of momentum of the fluid as it moves past the cylinder. This is the basis of the **wake survey method**.

The total drag (form + viscous) can be measured by calculating the rate of loss of momentum of the fluid as it goes past an obstacle. This involves velocity and pressure measurement in the wake of the object. The procedure described below has an advantage since it is valid for objects of any shape.

Consider flow past a cylinder placed in a wind tunnel as shown below (Figure 1):

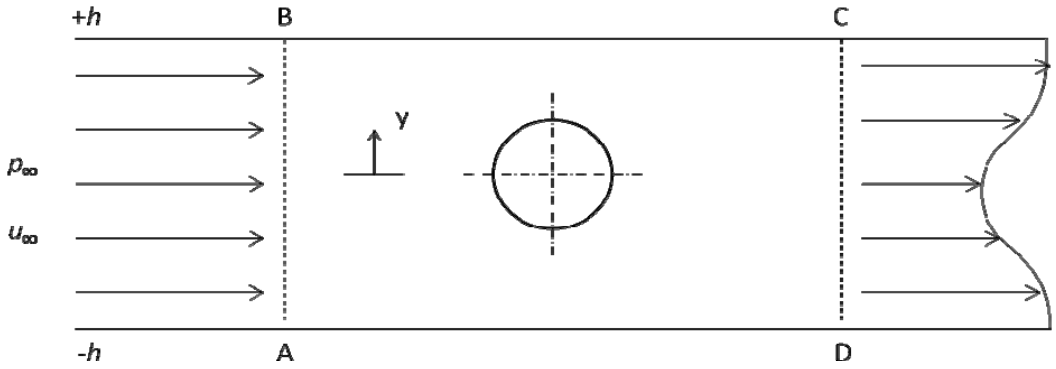

Figure 1: Configuration for wake survey method.

Subscript ∞ refers to approach (incoming) flow conditions and is also nearly equal to the conditions prevailing outside the wake. Making a momentum transfer calculation over the control volume ABCD we have (with M as momentum flux (time-averaged) per unit length of the cylinder).

$$M_{AB} = -\rho \int_{-h}^{h} U_\infty^2 dy$$

$$M_{CD} = \rho \int_{-h}^{h} U_1^2 dy$$

$$M_{BC+AD} = \rho \int_{-h}^{h} U_\infty (U_\infty - U_1) dy$$

where

$$\int_{-h}^{h} \left(U_\infty - U_1\right)\, dy$$

is the flow rate leaving the sides BC and CD. Hence, the force acting on the fluid medium contained in the control volume is

$$F = M_{AB} + M_{CD} + M_{BC+AD}$$

The external force has two components - one related to drag acting on the cylinder (D) and the second related to pressure drop in the tunnel over the length AD. Pressure drop effects are usually a small fraction of the momentum flux at high tunnel speeds. Experience shows that it needs to be included for free stream velocities less than 5 m/s. Hence, drag per unit length acting on the cylinder is

$$D = \rho \int_{-h}^{h} U_1 \left(U_\infty - U_1\right) dy + \int_{-h}^{h} (p_1 - p_2)\, dy \quad \text{and approximately} \quad D = \rho \int_{-h}^{h} U_1 \left(U_\infty - U_1\right) dy$$

The wake survey must be carried out at least $10d$ – $15d$ away from the cylinder so that regions of reversed flow are not encountered. The above integrals can be evaluated numerically using say, Simpson's rule. If the exit plane CD is sufficiently far away from the cylinder, the static pressure contribution is, once again, small. If the static pressure variation is significant across the wake, the tunnel static cannot be used for velocity measurement. Here, the following procedure is adopted.

Measure $\overline{p} = p_1 + \frac{1}{2}\rho U_1^{\,2} - p_{ref}$ as a function of y using a total pressure probe.

Measure $p_s = p_1 - p_{ref}$ as a function of y using a static pressure probe.

Compute $\frac{1}{2}\rho U_1^{\,2} = \overline{p} - p_s$

as a function of y and hence determine U_1. In the pressure integral, $p_s = p_1 - p_{ref}$ can be used as the integrand.

The static pressure probe consists of a hypodermic needle type pitot tubes. There is some uncertainty in locating the axis y=0 during the experiment. It is common practice to match the center of the cylinder and the tip of the probe. The typical dimensions of the pitot tube are, OD = 0.8 mm and ID = 0.5 mm.

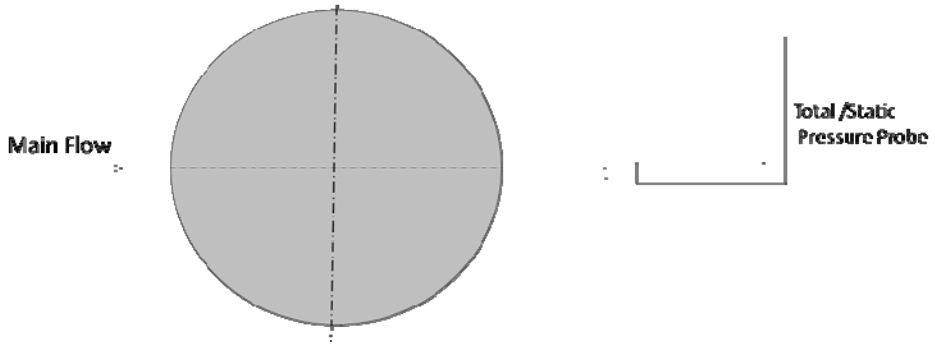

Figure 2: Schematic drawing showing the wake survey method

The goal of the experiment is to determine the time-averaged drag coefficient using the wake survey method. The data is to be generated for various wind tunnel speeds and a given size of the cylinder. The velocities and pressures appearing in above equations are time-averaged values. This averaging can be done on the digital manometer itself using time constant knob and waiting for sufficiently long time for the reading to stabilize.

Note that the wake survey method is independent of the shape of the object placed in the wind tunnel. Repeat measurements when the cross-section is a symmetric aerofoil at zero angle of attack. Compare the observations recorded and their respective drag coefficients.

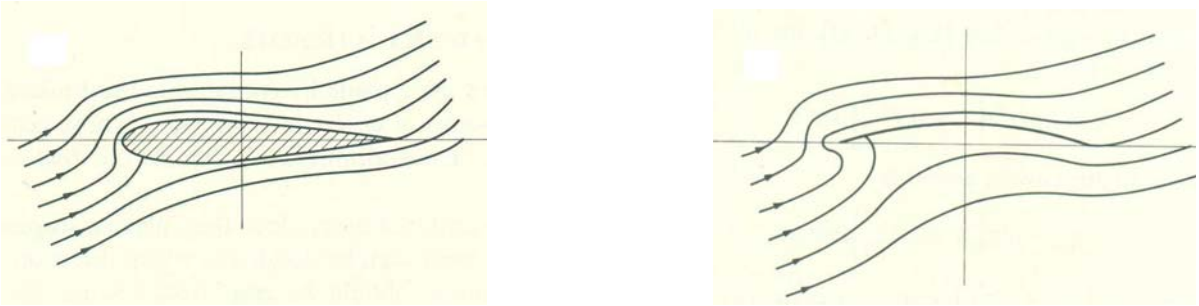

Figure 3: An object with an aerofoil shaped cross-section; left: symmetric aerofoil with flow at an angle of attack; right: circular arc aerofoil of zero thickness.

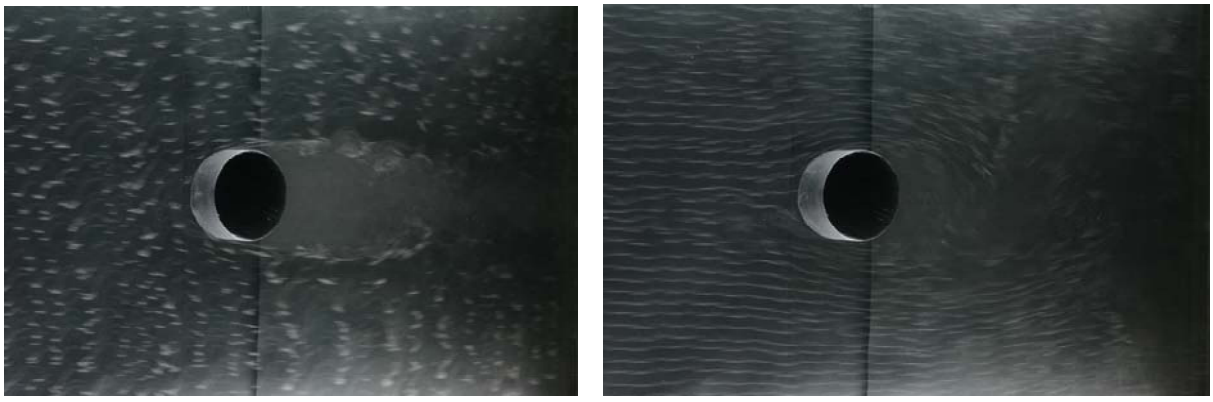

Figure 4: Smoke tunnel photographs of flow past a circular cylinder. On the left side, a near-steady circulation pattern at lower tunnel speeds. At higher speeds, alternate shedding of vortices commences and makes the overall flow unsteady.

EXPERIMENT 3: Energy loss measurements in subcritical and supercritical open channel flow

High speed gas flow occurs in several practical applications such as supersonic flight of aircraft and nozzles and diffusers used in turbomachinery. The study of high speed gas flow in a laboratory tends to be expensive since it is accompanied by a large pressure drop. The following result, called *hydraulic analogy*, becomes useful in this context.

One can establish mathematically that the Navier-Stokes equations in one-dimensional inviscid flow have identical form, whether applied to compressible gas flow or to shallow open channel liquid flow. This result, however, requires that $\gamma = C_p / C_v$, for the gas be equal to 2.0. The two flow systems – inviscid compressible gas versus shallow open liquid flow, are mathematically analogous. Since, no real gas has $\gamma = 2$, the analogy is only qualitatively valid. However, it is useful in studying shock fronts, which form in high speed gas flow. This is because shocks, when formed in at a liquid surface, are visible to the naked eye, whereas they remain unseen in a gas till special optical methods are employed. Further, the energy requirement to run a liquid flow experiment is minimal in comparison to gas. Hence, the analogy permits a simple way for studying energy losses in gas flows.

The criterion for gas flow to be classified as compressible is

$$\frac{u}{c} > 0.3$$

where c is the speed of sound in the gaseous medium. Open channel flow can be classified as shallow if the wavelength of a disturbance propagating on its surface is much larger than $h(x)$. In general, a disturbance will consist of a superposition of waves, each one which need not satisfy the shallow channel criterion. The analogy being studied here requires that the channel be shallow over the entire range of wavelengths. (It is also a source of error since it is difficult to enforce this condition in an experiment, unless h is made very small).

The speed of propagation of infinitesimal disturbances in the body of a fluid is the speed of sound. For an ideal gas

$$c = \sqrt{\gamma p / \rho}$$

The speed of propagation of shallow water waves, called gravity waves, on the surface of a stationary liquid is given a symbol w and is given as

$$w = \sqrt{gh}$$

Hence, speed of sound c and the speed of gravity waves w are analogs of each other. The ratio u/c, where u is fluid velocity is called Mach number, and given the symbol M. The ratio $Fr=u/w$ is called the Froude number. We have

$M < 1$ subsonic flow
$M = 1$ sonic flow
$M > 1$ supersonic flow

Similarly

$Fr < 1$ subcritical flow
$Fr = 1$ critical flow
$Fr > 1$ supercritical flow

The possibility of discontinuities propagating in the gaseous flow arises if $M > 1$. A similar situation prevails in liquid flows for $Fr > 1$ and is called a hydraulic jump. Significant energy losses take place across a jump.

A shallow, open channel liquid flow arrangement is shown in Figure 1. The flow is driven by a gravity head h (x). The variables of this problem are u, p, h and b where b is the channel width. The variation in surface elevation is created by an adjustable gate. Surface elevations are measured by using a micrometer arrangement.

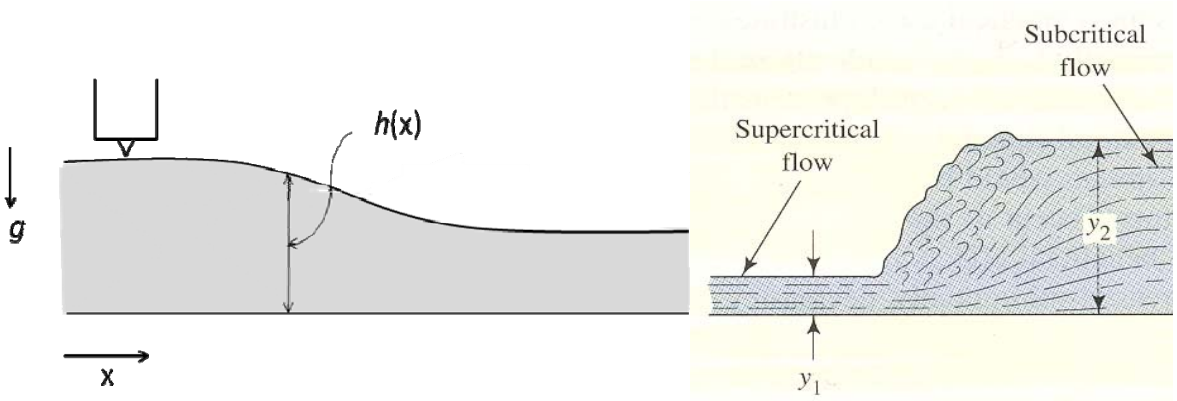

Figure 1: Nomenclature for open channel flow; left: subcritical flow everywhere; right: approaching flow from the left is supercritical giving rise to a hydraulic jump.

The goals of the present experiment are as follows:

a. For a given position of the gate, map the surface profile of the liquid layer.
b. Calculate the energy loss between two suitably chosen sections (upstream and downstream) of the channel.
c. Change the gate position and repeat part (b).
d. Plot the dimensionless energy loss as a function of the Froude number just downstream of the gate. Include data for experiments in which Froude number varies from below unity to above unity. Record specific observations when the Froude number (anywhere) exceeds unity, giving rise to a hydraulic jump. Record and report images where possible.

Remarks: Losses can be calculated from the energy equation applied between the inflow (1) and outflow (2) stations, namely

$$\text{losses} = e_2 - e_1 = \{ g(H_2 - H_1) + \frac{u_2^{\,2} - u_1^{\,2}}{2} \} < 0 \qquad \text{where } e = \frac{p}{\rho} + \frac{u^2}{2} + gz$$

This expression of total energy accounts for pressure, kinetic energy and the gravitational potential.

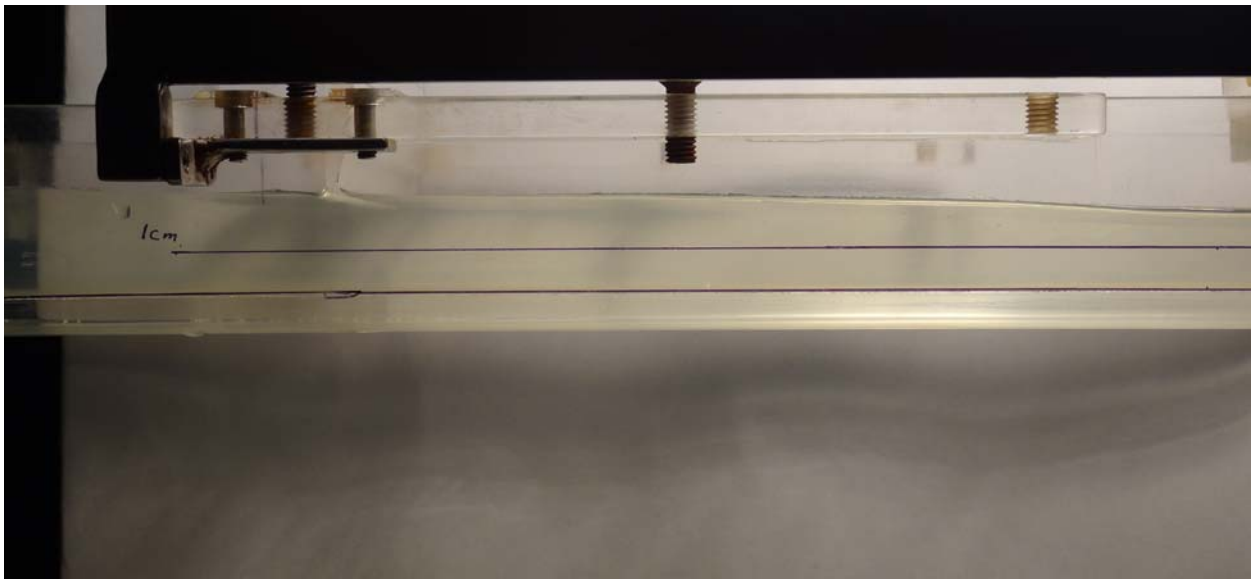

The photograph shows an example of *subcritical* flow. Flow direction is from left to right. Note that flow depth decreases monotonically in the flow direction. It can be shown that Froude number is less than unity over the distance considered.

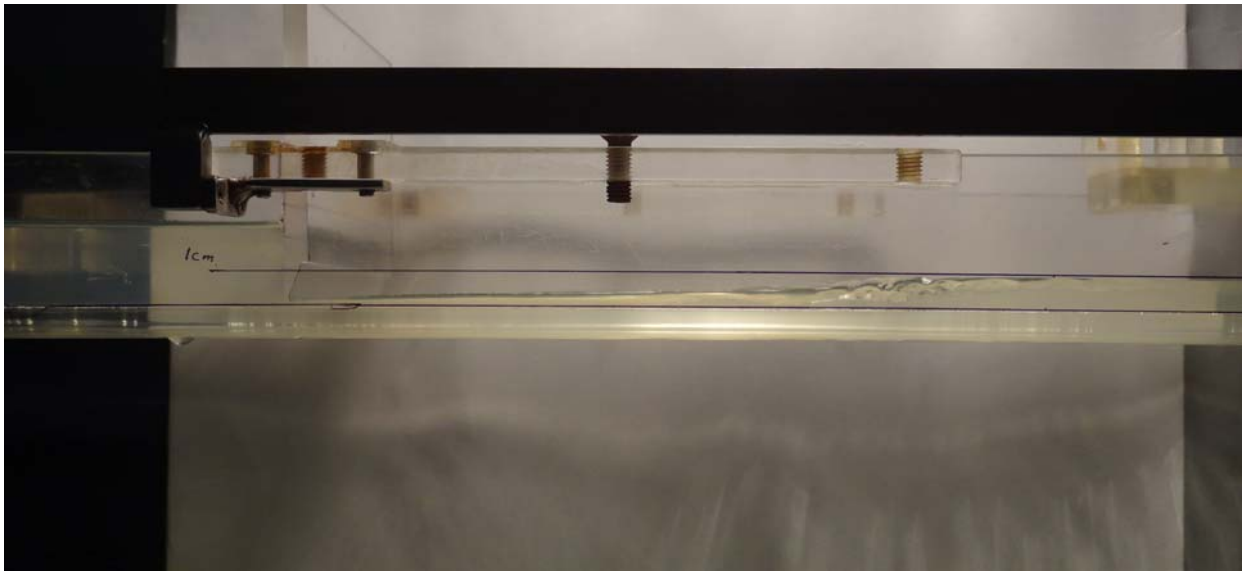

The photograph shows an example of *supercritical* flow. Flow direction is from left to right. Note that flow depth increases abruptly in the flow direction. It can be shown that Froude number is greater than unity upstream of the hydraulic jump. Flow is subcritical beyond the jump.

When a sharp edged object is placed in supercritical flow ($Fr > 1$), oblique shocks emanating from the upstream corner will form. When a rounded object such as a cylinder is placed in supercritical flow, a bow shock is to be seen. The bow shock is close to the object upstream but is not attached to it. See photographs below. Flow is from left to right and the photograph is a plan view. The disturbances on the right side of the photograph are related to the hydraulic jump.

WEDGE

CIRCULAR CYLINDER

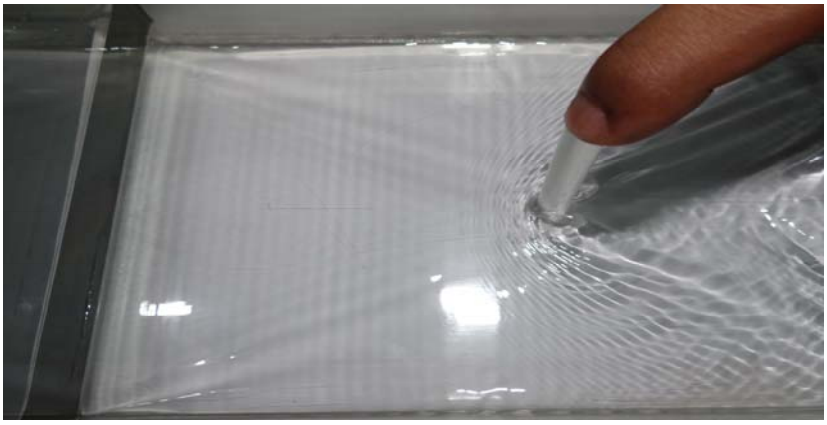

It can be readily confirmed that shocks do not form in subcritical flow, for example, post the hydraulic jump.

EXPERIMENT 4: Measurement of fluid viscosity

(a) Method of Stokes Law for Drag

Under low speed attached (unseparated) flow conditions, the drag acting on an object of spherical shape is given by *Stokes' Law*

$$D = 3\pi U d \mu$$

where U is the approach velocity of the fluid (or the velocity of the object relative to a stationary fluid), d is particle diameter and μ is dynamic viscosity of the fluid medium. Stokes' law is valid if

$$\mathrm{Re} = \frac{\rho U d}{\mu} < 1$$

For a spherical object falling in a gravity field, the object at zero velocity accelerates to a *terminal* velocity when drag becomes equal to weight. The net force acting on the sphere is then zero and its velocity remains unchanged with distance. Under these conditions, we have (including buoyancy)

$$D = mg\left(1 - \frac{\rho_f}{\rho_s}\right)$$

where ρ_f is the fluid density and ρ_s is the density of the spherical particle. This equation can be used to determine dynamic viscosity μ. The constraint, Re < 1 is accomplished by a suitable choice of the sphere diameter.

For a wider range of Reynolds number, namely Re < 5, Stokes' law can be extended to the form

$$D = 3\pi U d \mu \left(1 + \tfrac{3}{16}\mathrm{Re}\right)$$

This formula is called *Oseen's approximation*.

In part (a) of the experiment, spheres made of aluminum, mild steel and plastic beads of various diameters are dropped in a long column containing SAE 40 oil. Each sphere is allowed to move a certain distance before its velocity has become equal to the terminal velocity. The terminal velocity is measured by noting the time it takes for the sphere to move a predetermined distance. Time is measured using a photodiode arrangement. Liquid density is measured using a weighing balance. The following data can be used:

$\rho_{\text{steel}} = 7.75$ gm/cm^2, $\rho_{\text{Al}} = 2.78$ gm/cm^2. For plastic beads, weight must be measured to calculate the density of the material.

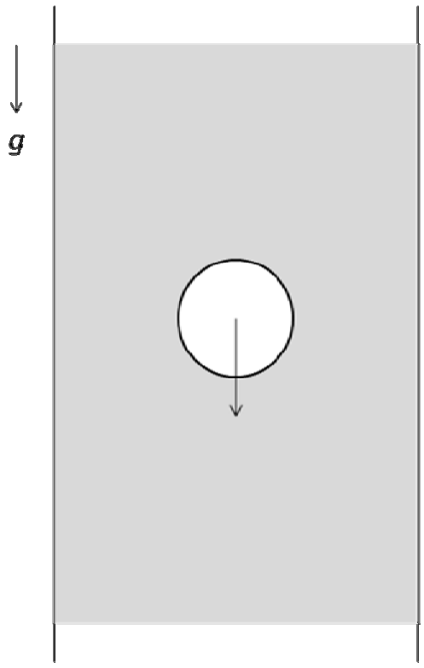

Figure 1: Viscosity measurement using Stokes law of drag acting on a spherical particle.

Viscosity may also be measured by dropping objects through the liquid column, which are not necessarily spherical in shape. For example, one may use the formula for drag acting on a cylinder of length *L* as

$$D = \frac{4\pi\mu UL}{\frac{1}{2} - \gamma - \log\frac{\mathrm{Re}}{8}}$$

where γ is Euler's constant (0.577. .).

This formula is also valid only for small Reynolds numbers, Re<1. Note that drag is only a weak function of diameter for a circular cylinder.

(b) Rotating Cup Viscometer

The viscometer measures liquid viscosity using the following principle. Consider two concentric cylinders, the space between which is filled with the liquid of unknown viscosity. The outer cylinder is given an angular velocity ω, while the inner cylinder is stationary. Provided Re, defined as $\rho\omega(R_2 - R_1)^2/\mu$ is not large,

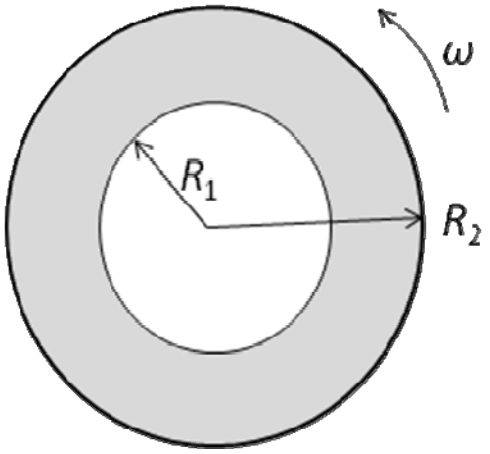

Figure 2: Viscosity measurement using a rotating cup viscometer.

one dimensional motion prevails in the annular region, with flow only in the angular direction. Navier-Stokes equations can be analytically solved for this flow arrangement. Torque per unit length of the inner cylinder is given by

$$\frac{T_q}{L} = \frac{4\pi\mu\omega R_1^2 R_2^2}{\left(R_2^2 - R_1^2\right)}$$

If T_q can be measured, μ can be obtained from this formula. [Note: R_1=1.5cm, R_2=3.5cm in the experimental apparatus.]

The viscometer to be used in part (b) of this experiment consists of the following arrangement.

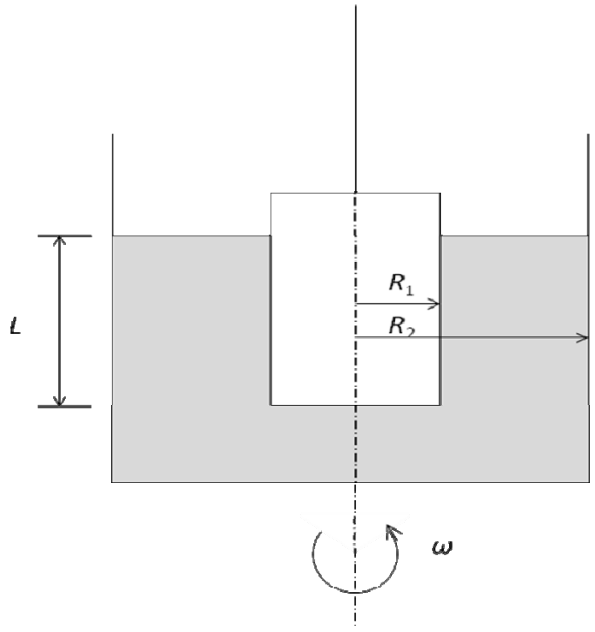

Figure 7: Schematic drawing of a Rotating Cup Viscometer.

The outer container is rotated at a constant angular velocity (ω), which can be measured using a stopwatch. The inner cylinder is suspended by a thin wire of known torsional spring constant (say, k = 0.08109gm$_f$.cm/div). The angular deflection of this wire is measured on a scale and torque acting on the inner cylinder is calculated as

$$T_q = k\theta$$

For small depths of immersion (i.e., small L), μ will depend on L due to edge effects. As L increases, μ becomes independent of L. The curve μ vs L, is required to be plotted. The viscometer has a water bath which can be used to heat oil. Determine μ as a function of temperature up to 50^{o}C. Plot μ as a function of temperature T and determine the constant C and exponent n in the empirical expression

$$\frac{\mu}{\mu_o} = 1 + C\left(\frac{T - T_o}{T_{\max} - T_o}\right)^n$$

where T_o is the room temperature. Express μ in units of kg/m-s.

Remark: The lower surface of the rotating cylinder will also contribute to the total torque acting on the torsional wire. Using a one-dimensional model, develop an expression for this quantity. Examine its contribution to the total torque for varying values of the depth of immersion, L. {It is likely that, with this correction, the dependence of viscosity on the immersion length is completely accounted for.} A second approach: measure angular deflection with zero immersion length when the inner cylinder just touches the surface of the liquid. Subtract this contribution in subsequent calculations when the inner cylinder is immersed to a greater extent. If the zero immersion length experiment is hard to conduct, the limiting torque can be determined by progressively reducing the immersion length from 10, to 5, to 2mm.

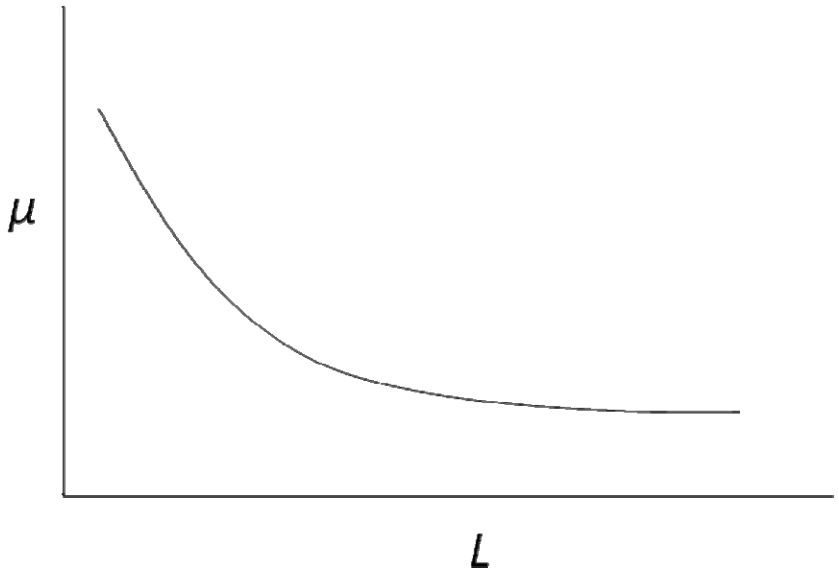

Figure 3: Variation of measured viscosity with the depth of immersion when the annular flow model is used for the torque developed

(c) Measurement of Air Viscosity

For fully developed laminar flow of air (viscosity μ) through a circular tube of diameter d, the pressure gradient is a constant and related to the mean flow rate Q according to the formula

$$-\frac{dp}{dx} = \frac{128\mu Q}{\pi d^4}$$

Hence the knowledge of Q, $-\frac{dp}{dx}$ and d from experiments will determine the dynamic viscosity.

In this experiment, the suction side of a blower draws air through a long tube. Pressure taps located on the tube surface determine the pressure drop along its length. The mean flow rate is measured using a rotameter.

In the early part of the tube, pressure gradient is not a constant due to flow development effects. A typical pressure profile is shown below.

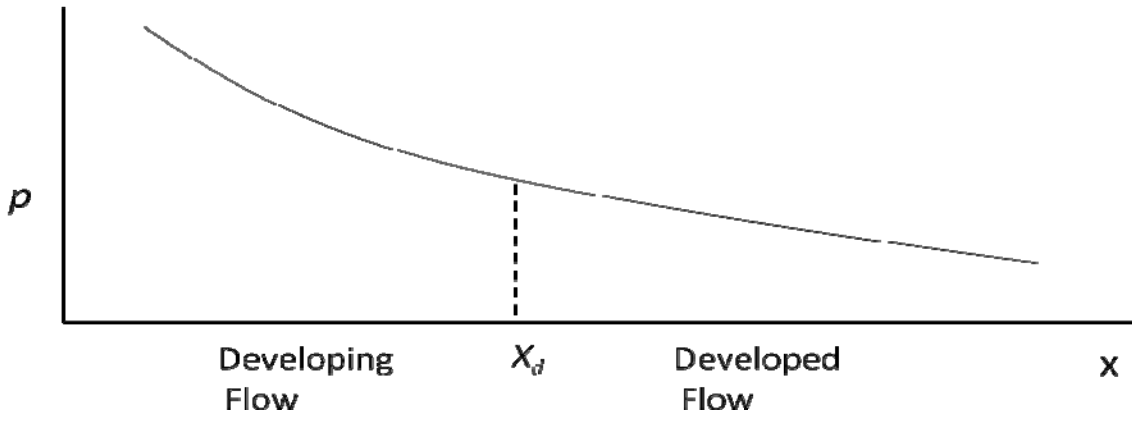

Figure 4: Variation of pressure with distance in developing and fully developed flow in a tube.

Pressure is measured using a scanning valve and a digital manometer. To determine viscosity μ, $\frac{dp}{dx}$ must be determined beyond the development length x_d. The rotameter is calibrated at 21°C and hence its reading must be corrected for room temperature changes. Determine μ at three different values of the flow rate Q.

EXPERIMENT 5: Determination of friction factor as a function of Reynolds number in pipe flow

Friction factor, a major quantity of importance in engineering is defined as

$$f = \frac{(p_1 - p_2)/L}{\frac{1}{2}\rho U^2/d}$$

Here, the symbols have their usual meaning. The numerator is pressure drop per unit length of the tube, U is the average fluid speed, and d is diameter. Friction factor is known to be a function of Reynolds number and surface roughness of the tube. This information is summarized in the form of Moody's charts (reproduced on the next page). Reynolds number is defined as

$$\mathrm{Re} = \frac{\rho U d}{\mu}$$

The relative roughness (with rms value k) of the tube surface is expressed in dimensionless form as

$$\varepsilon = \frac{k}{d}, \text{ being zero for a smooth tube.}$$

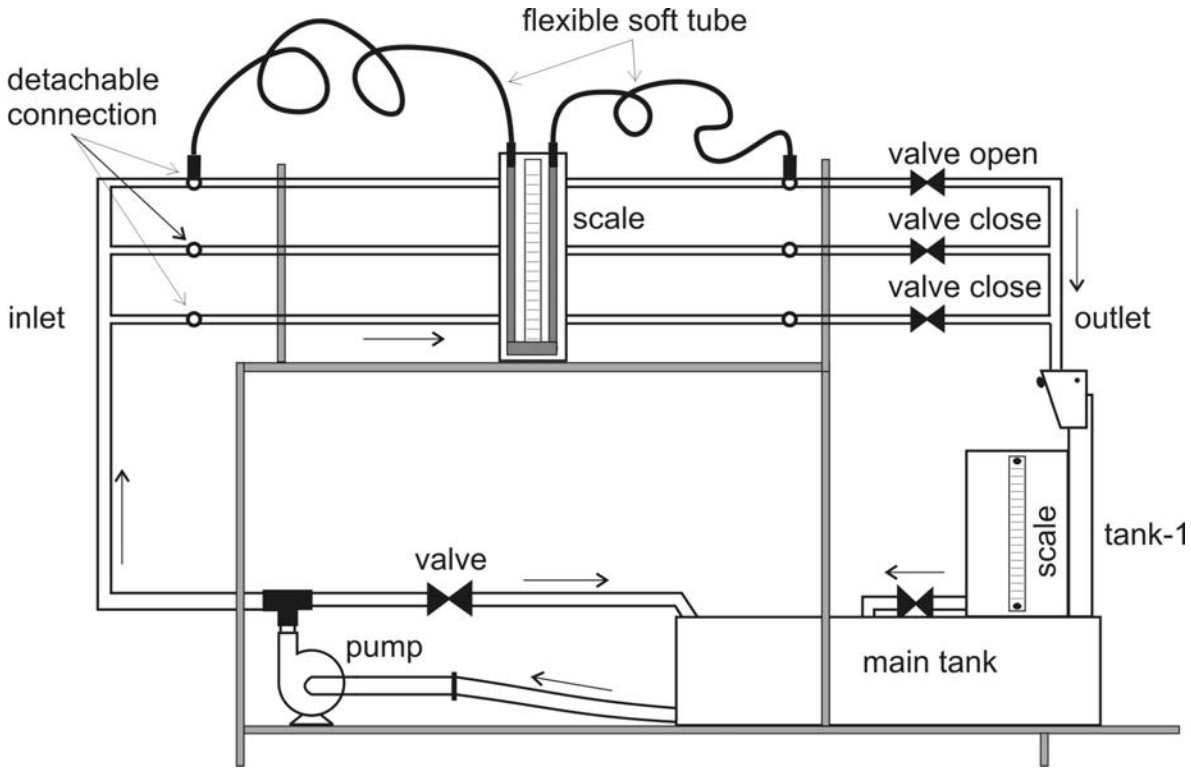

Figure 1: Experimental setup for friction factor measurement in tubes.

The present experiment is aimed at plotting friction factor as a function of Reynolds number for smooth tubes of various diameters.

The apparatus consists of a pipe circuit through which several GI pipes of 15, 20, 25, and 32 mm diameters are provided. The flow rate can be varied over a range of values. One pipe of brass of 25 mm diameter is also available. Each pipe is provided with two pressure tappings a certain distance apart. A U-tube differential manometer is provided to find the pressure difference between two tappings. The tappings may be connected to the manometer one after the other. A collecting tank is used to find the discharge of water through the pipes.

Note that brass surface is smooth while the GI tubes are rough whose roughness can be estimated from engineering handbooks

The goals of the experiments are the following.

i. Measure flow rate and pressure drop for the tubes given.
ii. Express the measurement data in terms of friction factor and Reynolds number.
iii. Superpose these values on Moody's diagram.

Interpret the results obtained.

Remarks

i. Calculate pressure drop from the mercury-in-glass manometer as

$$p_1 - p_2 = (\rho_{\text{mercury}} - \rho_{\text{water}})gH$$

ii. Account for the shape of the meniscus formed when mercury is in contact with water.
iii. Since the flow is turbulent, pressure changes are time dependent but are damped by mercury of the manometer. Wait for some time so that only time-average readings are recorded.
iv. In calculations, use fluid properties evaluated at the room temperature.

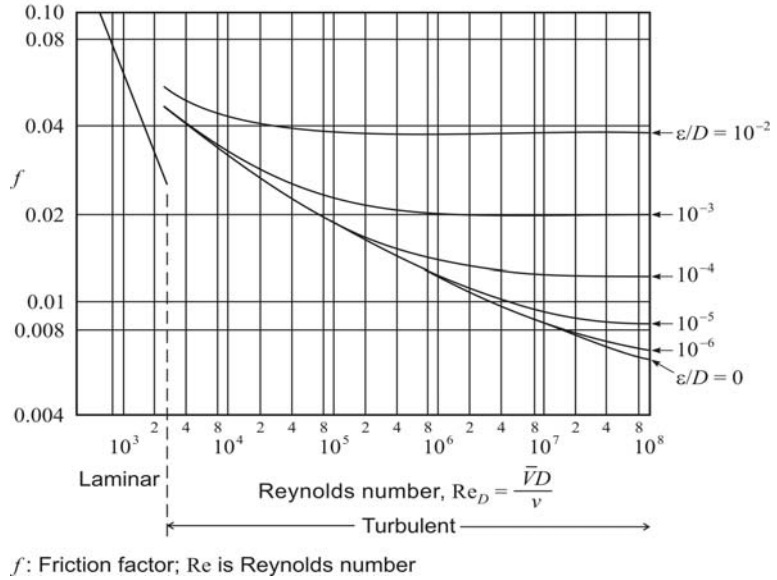

Figure: Moody's chart (Friction factor versus Reynolds number) for flow in a tube

EXPERIMENT 6: Studying laminar-turbulent transition for flow in a tube

Laminar flow in a tube is known to undergo transition to become turbulent with increasing values of Reynolds number. The two states of flow can be distinguished by introducing a color dye along the axis of the tube. In laminar flow, the dye remains undisturbed and moves along the tube axis. In turbulent flow, the velocity field reveals time dependent oscillations which lead to stronger mixing of the dye with the surrounding fluid.

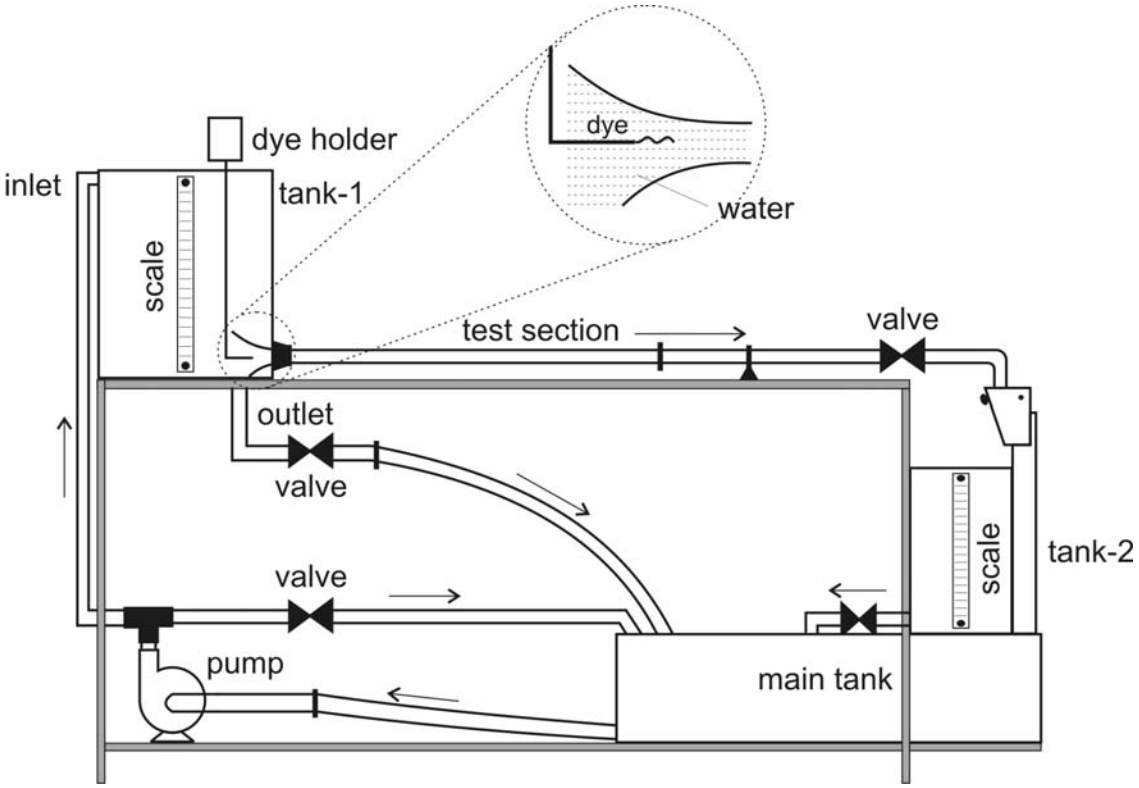

Figure 1: Reynolds Apparatus for demonstrating laminar and turbulent flow

The apparatus consists of a storage and supply tank, which has the provision for supplying color dye through a jet. A perspex tube is provided to visualize the flow condition within the tube. The entry of water in the perspex tube is through an elliptical bell mouth to ensure smooth flow at the entry. A regulating value is provided downstream to regulate the volumetric flow. Vary the discharge gradually to prevent flow disturbances, particularly in the transition range of Reynolds numbers.

A collecting tank is used to measure discharge of water through the tube.

The goals of the present experiment are as follows:

i. Visualize dye mixing for flow in a tube under laminar and turbulent conditions.

ii. Carefully estimate the critical Reynolds number below which flow is laminar and above which it is turbulent.

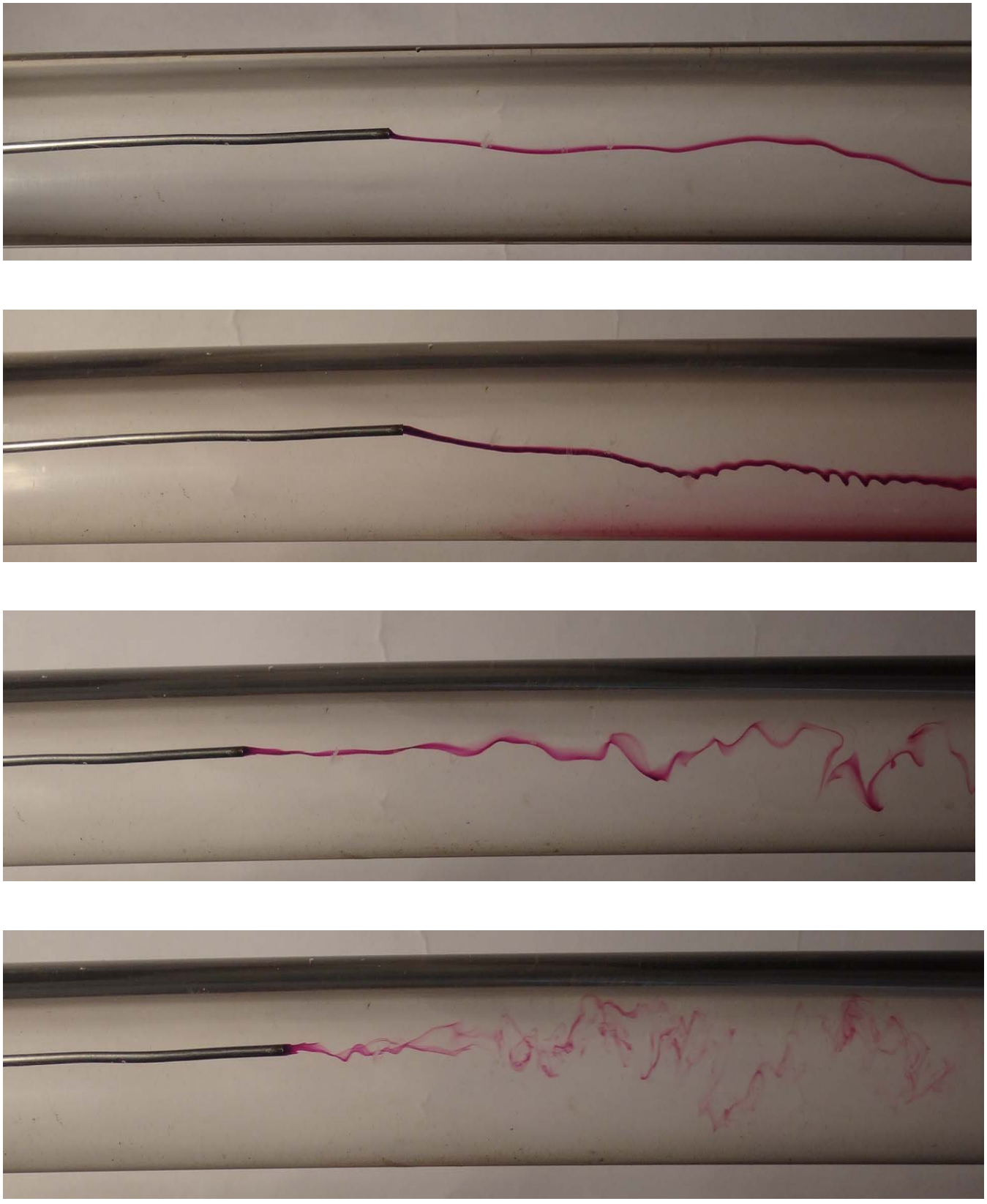

Sequence of dye traces introduced in a tube with increasing Reynolds number (top to bottom).

EXPERIMENT 7: Pressure distribution around a circular cylinder in high Reynolds number flow

Cylinders of varying diameter (d = 25.4 – 61 mm) are placed in a low speed wind tunnel. The force acting on them consists of viscous drag and form drag, the latter being predominant if flow separates on the surface of the cylinder. The wind tunnel provides velocities up to U = 15 m/s and for a diameter of 50 mm, the corresponding Reynolds number $=\rho Ud/\mu$ is 4.8×10^5. For a cylinder the laminar separated regime extends over $50 < \mathrm{Re} < 5\times10^5$. Hence for the diameters and velocities studied here, the boundary-layer over the cylinder is expected to be laminar.

In separated flow the total drag consists of form and viscous drag but the former is considerably larger in proportion. Form drag arises from an asymmetric distribution of surface pressure on the forward and rear halves of the cylinder and hence can be measured. It constitutes a representative value for the total drag. A typical pressure distribution over the cylinder is shown in Figure 1.

For potential flow, coefficient of pressure is given as

$$Cp = \frac{p - p(\text{tunnel})}{\frac{1}{2}\rho U^2} = 1 - 4\sin^2\theta$$

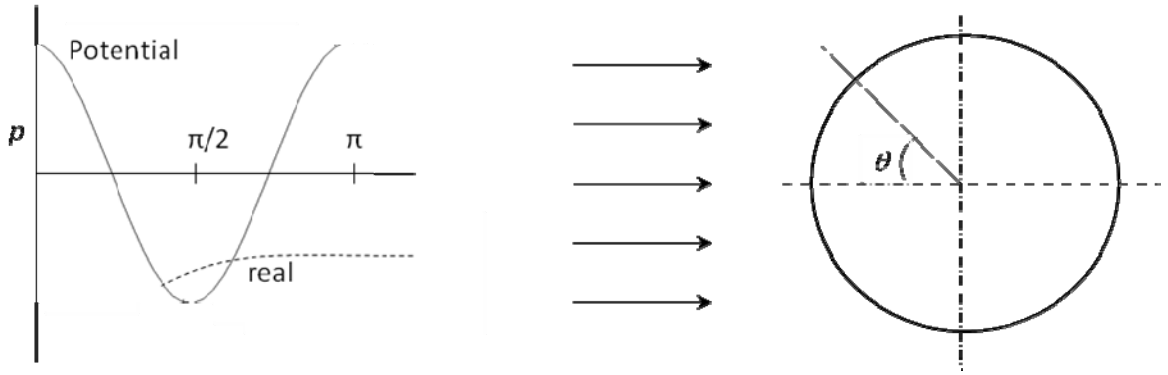

Figure 1: Inviscid and rea1 pressure distribution around a cylinder.

Forces under discussion are time-averaged values. Accordingly, the measurements of pressure and velocity are also time-averages.

In this part of the experiment a single pitot tube embedded within a circular cylinder measures pressure distribution $p(R,\theta)$ (static pressure as a function ofθ at r= R, the cylinder surface) where R is the radius of the cylinder and θ corresponds to the angular location on the cylinder surface. Angle θ can be varied by turning the position of the cylinder relative to the main flow. In the figure shown below, OA is the pitot tube, which senses the local surface static pressure.

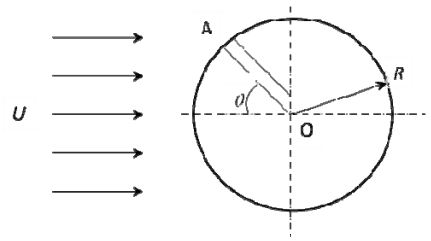

Figure 2: Measurement of pressure over the cylinder surface.

With the knowledge of $p(R,\theta)$, form drag per unit length acting on the cylinder is calculated as

$$D = \int_0^{2\pi} p(R,\theta) R \cos\theta \, d\theta = 2\int_0^{\pi} p(R,\theta) R \cos\theta \, d\theta$$

and the drag coefficient

$$C_D = \frac{D}{\frac{1}{2}\rho U^2 (2R)}$$

C_D must be determined for smooth cylinders for three different values of U (=5.0, 7.5, 10 m/s). The static pressure distribution is measured relative to the tunnel static pressure p_{tunnel} prevailing at that location. Since

$$\int_0^{2\pi} p_{tunnel} R \cos\theta \, d\theta = 0 \qquad \text{(constant } p_{tunnel}\text{)},$$

it need not be included in the formula for drag given above. Note that this approach does not include the contribution of viscous stresses to the total drag.

The goals of the experiment are:

a. determine the pressure variation over the cylinder in dimensionless form for a chosen Reynolds number
b. calculate form drag and form drag coefficient by integration
c. identify the point of boundary-layer separation.
d. Correlate the pressure distribution with flow visualization images recorded in the smoke tunnel, sample photograph given below.

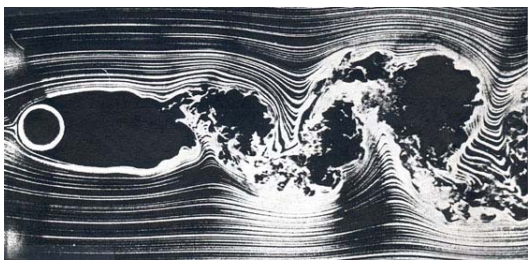

Figure 3: Smoke tunnel visualization of flow past a circular cylinder at high Reynolds number

EXPERIMENT 8: Boundary layer flow over a flat plate

In high Reynolds number flow (Re >> 1), a thin boundary-layer is formed over a solid surface. Viscous effects are confined within this layer (of thickness δ) and potential flow prevails outside it. At any position x, the boundary-layer is thin in the sense that

$$\frac{\delta}{x} << 1$$

The origin of flow separation in adverse pressure gradient and the phenomenon of turbulence can be traced to the existence of the boundary-layer. Hence it is of importance to measure velocity distribution in the neighborhood of the solid wall.

In the present experiment, a flat plate boundary-layer (Figure 1) is studied.

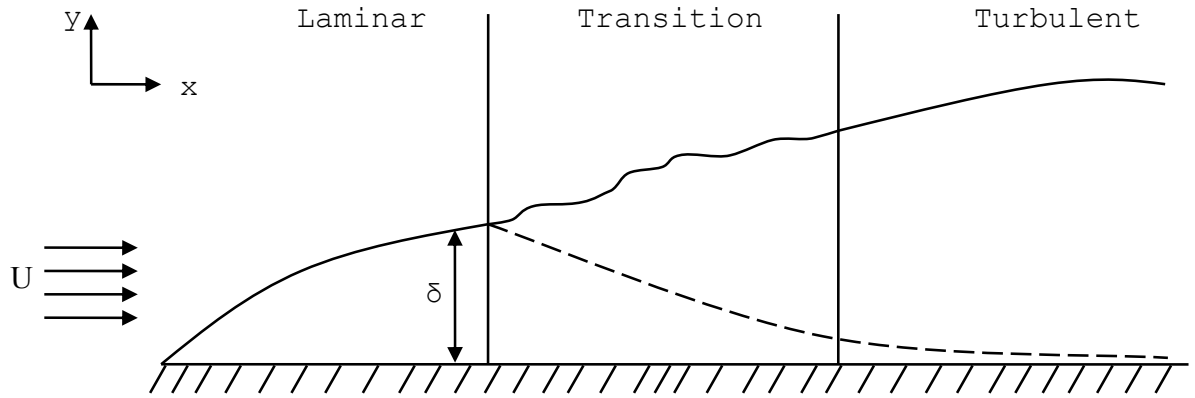

Figure 1: Regimes of Boundary-layer Flow over a Flat Plate.

Though a flat plate boundary-layer does not separate, it undergoes transition to become turbulent. The following limits are usually observed in practice.

$Re_x < 60000$ Laminar; $Re_x > 5 \times 10^5$ Turbulent

The theoretical solutions for velocity profiles in a flat plate boundary-layer are as follows:

Laminar: $$\frac{u}{U} = \frac{y}{\delta}\left(2 - \frac{y}{\delta}\right) \qquad (1)$$

where

$$\frac{\delta}{x} = \frac{5}{\sqrt{\mathrm{Re}_x}}, \qquad \mathrm{Re}_x = \frac{Ux}{\nu}$$

Turbulent: $$\frac{u}{U} = \left(\frac{y}{\delta}\right)^{1/7} \qquad (2)$$

where

$$\frac{\delta}{x} = \frac{0.371}{\mathrm{Re}_x^{0.2}}$$

In the experiment, a hypodermic needle–type pitot tube and a digital manometer are used to measure velocity. The experimental procedure is as follows.

(i) Traverse the pitot tube above the plate to estimate the boundary-layer thickness. This is easily done since $u \to U$ as $y \to \delta$, the outer edge of the layer.

(ii) Divide the estimated thickness in 10 parts. The probe can be moved back towards the plate, in these increments, with the help of a micrometer arrangement.

(iii) Repeat steps (i) and (ii) at for the laminar and turbulent portions of the boundary-layer.

The state of flow as laminar or turbulent can be judged either based on the criterion of the local Reynolds number or by examining the shape of the velocity profile. Typical profiles in laminar and turbulent flow are shown in Figure 2.

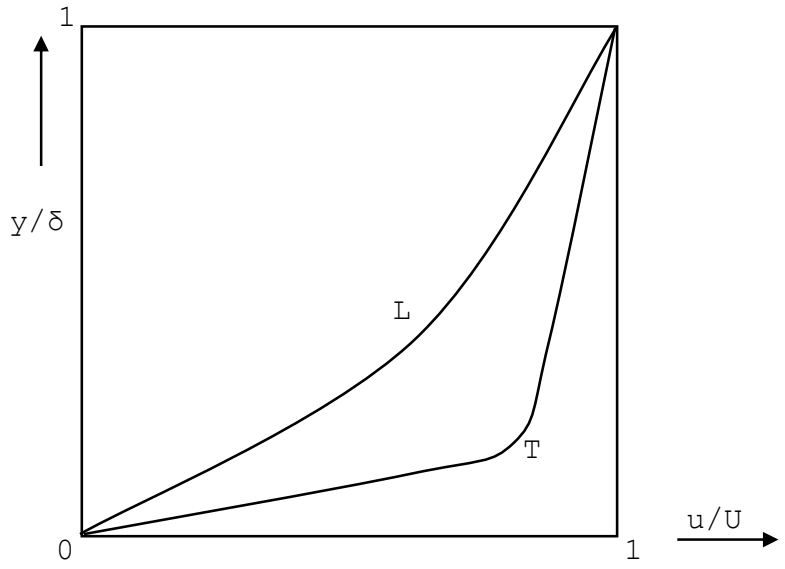

Figure 2: Laminar (L) and Turbulent (T) Velocity Profiles in a Flat Plate Boundary-layer

The experimentally determined profiles must be compared to the theoretical results given by Equations 1 and 2.

The digital manometer is calibrated for velocity measurement at 18^{o}C. At all other temperatures a correction factor must be applied. The required correction graph is available in the laboratory.

The above experiment can be repeated with a rough flat surface to observe the following:

(a) drastic increase in boundary-layer thickness δ and
(b) near constancy of $\delta(x)$ with the streamwise coordinate.

Interpret these results.

Useful references

1. T.G. Beckwith and N.L. Buck, *Mechanical Measurements*, Addison-Wesley, MA (USA), 1969.
2. H.W. Coleman and W.G. Steele Jr., *Experiments and Uncertainty Analysis for Engineers*, Wiley & Sons, New York, 1989.
3. E.O. Doeblin, *Measurement Systems*, McGraw-Hill, New York, 1986.
4. R.J. Goldstein (Editor), *Fluid Mechanics Measurements*, Hemisphere Publishing Corporation, New York, 1983; second edition, 1996.
5. B.E. Jones, *Instrumentation Measurement and Feedback*, Tata McGraw-Hill, New Delhi, 2000.
6. D.C. Montgomery, *Design and Analysis of Experiments*, John Wiley, New York, 2001.
7. A.S. Morris, *Principles of Measurement and Instrumentation*, Prentice Hall of India, New Delhi, 1999.
8. D.V.S. Murty, *Transducers and Instrumentation*, Prentice Hall of India, New Delhi, 1995.
9. D. Patranabis, *Principles of Industrial Instrumentation*, Tata McGraw-Hill, New Delhi, 1988.
10. C.S. Rangan, G.R. Sarma and V.S.V. Mani, *Instrumentation: Devices and Systems*, Tata McGraw-Hill, New Delhi, 1997.
11. M. Van Dyke, *An Album of Fluid Motion*, The Parabolic Press, California, 1982.